ACCEPTED MANUSCRIPT

Leaky waveguide deflector for 40 GS/s and 6 bits all-optical analog-to-digital converters

Massinissa Hadjloum[a*], Mohammed El Gibari[a], Hongwu Li[a], Afshin S. Daryoush[b]

[a] *Lunam Université, Université de Nantes, UMR CNRS 6164: Institut d'Electronique et de Télécommunications de Rennes, Faculté des Sciences et Techniques, 2 Chemin de la Houssinière, BP 92208, 44322 Nantes cedex 3, France*
[b] *Dept. of ECE, Drexel University, Philadelphia, PA 19104, USA*

Abstract

Analog-to-digital converters (ADC) are an important part of realizing direct digital receivers in future communication systems, where broad bandwidth, high effective number of bits, and low DC power consumption are an important requirement of achieving it at microwave frequencies. Due to a number of physical limitations of electrical ADC, design of an all-optical analog-to-digital converter (AOADC) is pursued and presented here based on highly stable mode-locked laser based clock signal pulses for optical sampling, and a combination of leaky waveguide optical deflector using electro-optical (EO) polymers and stationary optical windows followed with high-speed photodetectors as optical quantizer. The reported principle of the AOADC is to convert a broadband RF signal into a spatially sampled light using optical deflection angle variation before quantizing it using either binary or Gray coded optical windows. The design and modeling of an AOADC working up to 20 GHz RF frequencies (with Nyquist sampling rate of over 40 GS/s) and for providing a resolution of better than 6 bits with under 4W of power consumption. Performance is currently limited by both optical and microwave attenuation in the available EO polymers.

Keywords: All-optical analog-to-digital converter; Electro-optical polymer; Leaky waveguide; GS/s optical sampling; Bits of resolution

* Corresponding author. Tel.: 00 33 251125535. E-mail address: massinissa.hadjloum@univ-nantes.fr (M. Hadjloum).

Accepted manuscript

1. Introduction

Telecommunications and microwave imaging systems performance is enhanced by digital signal processing functions [1] and in particular direct digital receivers are target of broadband signal detection using an array of signal processed detection such as FFT (Fast Fourier Transform). Fast ADCs are required to cope with the increase of the transmission rate and/or the carrier frequency in the range of several tens of GHz.

Electronic ADCs are running today at constantly higher sampling rate. In recent years, Fujitsu Inc. introduced their second generation ultra-fast ADC in CMOS technology operating with sampling rate up to 65 GS/s. However, the ADC is constructed from many interleaved elementary ADCs [2], resulting in very high complexity and effective number of bits (ENoB)

ACCEPTED MANUSCRIPT

limitation of the ADC due to matching problems between interleaved elementary ADCs. As fundamentally, electronic ADCs ENoB is limited by the aperture jitter in electronic clocks and ambiguity in comparators, for elementary electronic ADCs to the state of the art with sampling rate of 12 GS/s, the resolution is limited to 5 bits [3].

Photonic ADCs can achieve much higher sampling rate and ENoB thanks to mode-locked-laser with an aperture jitter 4 to 5 times smaller than electronic clocks [4] and repetition rate over 160 GHz [5] for optical sampling. Compared with electronic ADCs, AOADCs performs both sampling and quantization in optical domain, as opposed to hybrid designs where sampling is done in optical domain while quantization is performed in electrical domain [6]. Our design approach relies on using spatial sampling by transferring the amplitude of the sampled RF signal to deflection angle using a leaky waveguide optical deflector [7]. The optical deflector operates based on principle of an electro-optical (EO) polymers as waveguiding core of leaky waveguide structure. The EO polymers are more attractive over LiNbO3 and other ceramics because of a closer velocity matching [8] between optical and RF waves with a stronger EO coefficient [9]. Moreover, the selected EO material has reported bandwidth of over 100 GHz [10]. Recent progress in chromophore synthesis allows obtaining polymers with EO coefficient up to 350 pm/V [9] that also meets board bandwidth due to the excellent velocity matching between microwave and lightwave signals. In addition, by combining the strong EO effect of the polymer with the very low timing jitters of actively mode-locked laser pulses [11], better conversion resolution, larger bandwidth and lower power consumption can be obtained than with electronic ADCs. These improvements are specific to optical solutions and makes AOADCs a very promising solution over electrical counterparts for 40 GS/s and effective number of bits (ENoB) of larger than 6 with low power consumption of under 4W.

In this paper, we present the practical architecture and design of both optical waveguide and microwave driving electrodes of a leaky waveguide optical deflector using EO polymers. Design challenges and performance optimization are introduced by taking into account realization constraints of a 40 GS/s AOADC [7, 9] meeting 6 ENoB of binary code and under 4W of power consumption. The paper presents the design topology of a leaky waveguide deflector and principles of achieving high angular deflection with a small angular divergence. Bandwidth constraints are addressed by analyzing both velocity mismatching and RF electrode attenuation by incorporating special design modifications.

Accepted manuscript

2. Operation principle of AOADC

The conceptual realization of AOADC is presented in Fig. 1, where it is composed of three main blocks [7]:

- A mode-locked laser provides short optical pulses of the order of picoseconds and pulse repetition interval of about 25 picoseconds (as minimum sampling time for Nyquist bandwidth of 20 GHz) a low timing jitter (of the order of 100 femtoseconds) for optical sampling of the applied RF signal to leaky waveguide based optical deflector.
- An optical deflector realized using an EO polymer in the region between RF electrodes to adjust deflection angle out of a leaky waveguide by converting each analog amplitude voltage variation of dV into an angular variation of dθ followed by a cylindrical lens to illuminate on the spatial coding mask.
- A stationary coding mask (in either binary or Gray codes) as optical windows for illuminating at a constant optical power level on an array of ultra high-speed photodetectors (with bandwidth

ACCEPTED MANUSCRIPT

of at least 40 GHz) to directly quantize the sampled RF signals, as 1 when illuminated and 0 when blocked off.

Since both mode-locked laser pulses with low jitters and quantization using array of photodiodes with optical masks have been already reported [7, 11], the leaky waveguide deflector remains the central element of the AOADC. The detailed cross sectional view of the optical deflector is depicted in Fig. 2, which is composed of an embedded coplanar strip line (CPS) that applies a broadband RF signal (designed for bandwidth of 20 GHz) to the EO polymer. The EO polymer forms an optical waveguide with a small leaky coefficient to the superstrate. The leaky coefficient is selected optimally to maximize propagation length along the leaky waveguide, while satisfying velocity matched bandwidth of at least 20 GHz between optical and electrical travelling waves. When pulses from the mode-locked laser propagate through the waveguide, part of the optical power leaks to the superstrate. A thin buffer layer in between EO waveguide and superstrate controls the amount of light leakage over the optical deflector length as the leaky coefficient. The effective deflection angle is being adjusted by EO changes in index of refraction of optical waveguide. The typical values of RF permittivity and optical index of refraction for various materials are highlighted in Fig. 2. The physical parameters of W, G, h_t and h_g are optimized for the performance compromise of bandwidth, power consumption, and effective number of bits (ENoB).

The leaky waveguide deflector of the AOADC has a structure similar to that of a conventional EO phase modulator (cf. Fig. 2), except that the top cladding (buffer layer) is thin enough, so a tail of the optical field extends into the superstrate with refractive index n_s. The index of refraction of n_s is selected to be greater than the effective core index of refraction of the optical waveguide to result in transfer of energy in the normal direction of substrate and superstrate interface. The leaked power will propagate in a direction normal to this interface and the power distribution along the length of leaky optical waveguide controls in far-field diffraction angle. Both the bandwidth and resolution of the optical ADC depend on the thickness of the buffer layer h_t, optical and microwave losses in the EO polymer since the optical distribution along the leaky waveguide are to be controlled.

The short mode-locked laser pulses with the low timing jitters are used for digital sampling of the applied RF signal. The sampling of RF signal is achieved by transforming applied RF signal to the leaky optical waveguide deflection angle. The travelling RF amplitude applied to the CPS results in changes in the effective refractive index of the poled EO polymer that is used as the waveguide core in the optical deflector. In particular, the applied RF signal induces this change due to a linear electro-optical (i.e., Pockels) effect, which effectively results in a change in deflection angle of θ, while satisfying Snell's law of refraction. The leaky wave is diffracted after propagation through superstrate-prism and is transmitted into the air at output angle of θ_o. The diffracted beam is focused by the cylindrical lens across an image line of the optical coding mask as optical windows. The opening of optical windows provides a constant optical energy on the array of high-speed photodiodes that are located behind each optical window. For an ENoB of $b=\log_2 N$, where N is the number possible states, b columns with N rows of optical windows are required with Nxb photodetectors arrays. Alternatively, Nxb fiber bundles could combine deflected light on each column of the optical window to a N:1 optical combiners that are remoted to a single ultra high-speed photodiode using parallel combination of optical fibers mounted behind the optical masks. The image line moves up and down, resulting in N distinct image lines, each one corresponding to an angle, according to an applied voltage as illustrated in Fig. 1.

The AOADC is designed for sampling rates f_s up to 40 GS/s and at least b=6 bits of resolution, with a very high resolution-sampling rate product of 2.56×10^{12} LSBs-Hz (where LSB means Least Significant Bits). In addition to the general advantages of all-optical ADCs, such as

Accepted manuscript

ACCEPTED MANUSCRIPT

high-rate sampling, transportation of the binary output signal and the sampling signal by optical fibers, and the resulting increased EMI immunity, the proposed architecture also offers [7] better immunity to optical noise because of a lesser sensitivity to the transmitted optical power fluctuations. Moreover, since all bit states are inputted by the same deflected optical power due to its spatial sampling operation and is not close to the shot noise limit in the photodetectors, a higher linearity for this ADC is expected. Finally by taking advantage of traveling wave electrodes of CPS, this AOADC exhibits an inherently high sampling rate and broadband modulation capability.

3. AOADC Effective Number of Bits (ENoB)

The bit resolution of the AOADC depends on the beam divergence angle $\delta\theta$, which is being controlled by optical distribution along length of the optical deflector and its leaky wave attenuation coefficient, and the total angular swing $\Delta\theta$ of the deflected beam. The $\Delta\theta$ depends on maximum voltage swing provided by the RF signal and the EO coefficient of the polymer. The number of resolved lines on the coding mask $N = \Delta\theta/\delta\theta$ is related to the number of bits of resolution, $b=\log_2 N$. For a given total angular swing of the deflected beam, one should reduce the leaky beam divergence to increase the resolution, so two conditions must be met:

- A single-mode optical waveguide. Indeed, multimode waveguide causes an enlargement of the deflected beam because of modal dispersion. The core width and height will be chosen according to the refractive index contrast between the core, the lower cladding and the buffer to obtain a single-mode waveguide.
- A large effective leaky waveguide length L_{eff} ensuring a small leaky beam divergence limited by the diffraction angle limit. The effective leaky waveguide length L_{eff} is controlled by the leakage coefficient α_f, in turn by the buffer layer h_t. A long effective length of the leaky waveguide requires a weak leakage meaning that the optical wave is still well confined in the waveguide core region and a small portion of it extends to the superstrate-prism.

The buffer layer thickness h_t is the key parameter to obtain the right leakage coefficient α_f. Fig. 3a shows its influence on α_f. The thicker is the buffer layer, the smaller is the leakage coefficient and larger is the effective leaky waveguide length, the smaller is the beam divergence, so the higher is the resolution. However, a long deflector length reduces the modulation bandwidth due to velocity mismatch of electrical and optical waves along the CPS and leaky wave optical waveguide. So, a design compromise is made between the resolution and the bandwidth of ADC. The initial optical leakage coefficient is considered between 0.1 and 0.3 Np/cm, corresponding to a buffer layer thickness 3.75 and 3.35 μm respectively, and an optimum effective waveguide length between 2 and 3 cm.

The optical waveguide structure has been designed and optimized for short optical pulses from a mode-locked laser at λ_o=1.55 μm using the software OptiBPM. The design assumes employing lower cladding and buffer layer (cf. Fig. 2) in polymer NOA63 ($n_g = n_t = 1.56$), core in EO polymer PMMI/CPO-1 (n_c=1.63), superstrate in a glass (n_s =1.7), resulting in an effective index n_{eff} =1.582. Optical attenuations over the all length of the leaky waveguide deflector is considered equal to 0.2 Np/cm (or 1.74 dB/cm). The single mode operation requirement leads to a waveguide core (cf. Fig. 3b) of 3-μm width and a 1-μm thickness, which meets the practical limits of low-cost micro-printing technique in the IETR laboratory.

Accepted manuscript

ACCEPTED MANUSCRIPT

By summing the contribution at each incremental segment of dz along the length of the waveguide to the optical leak wave and taking into account optical losses, the total leaky wave ψ at the deflection angle θ is expressed as:

$$\psi(\theta) = \int_0^L \alpha_f A e^{-(\alpha_f+\alpha_{opt})z} e^{-j(\beta-k_s \sin\theta)z} e^{-jk_s r}\, dz \quad (1)$$

Where

A: magnitude of the input lightwave in the waveguide at the origin z=0;

α_f: leakage coefficient;

α_{opt}: total optical losses due to material absorption and waveguide imperfection particularly the surface roughness;

β: phase propagation constant of the lightwave in the leaky optical waveguide;

k_s: wave number in the superstrate;

r: position vector at the observation point.

The effective refractive index of the waveguide is changed due to the Pockels effect of the core in electro-optical polymer as:

$$n_{eff} = n_{eff_0} + \Delta n = n_{eff_0} + \frac{1}{2} n_{eff_0}^3 r_{eo} \Gamma E(z) = n_{eff_0} + \frac{1}{2} n_{eff_0}^3 r_{eo} \Gamma E_o e^{-\alpha_{RF} z}$$

Where

n_{eff_0}: effective refractive index in absence of applied RF electrical field;

r_{eo}: electro-optical coefficient of EO polymer;

Γ: overlap integral between the RF and optical fields;

α_{RF}: microwave losses in the CPS line;

E(z): RF electrical field amplitude at z and expressed as $E_o e^{-\alpha_{RF} z}$ due to exponential decrease of RF field for a travelling wave, where E_o is the magnitude of the RF field at the input of the CPS line.

Similarly, the phase constant as function of the applied electrical RF field is:

$$\beta = k n_{eff} = k\left(n_{eff_0} + \frac{1}{2} n_{eff_0}^3 r_{eo} \Gamma E_o e^{-\alpha_{RF} z}\right) \quad (2)$$

where $k = \frac{2\pi}{\lambda_o}$ is the wave number in free space. By incorporating the Eq. (2) into Eq. (1), the total leaky optical field at the deflection angle of θ is then expressed as:

$$\psi = \alpha_f A e^{-jk_s r} \int_0^L e^{\{-(\alpha_f+\alpha_{opt})-jk(n_{eff_0}-n_s \sin\theta)\}z} e^{-j\frac{1}{2}kn_{eff_0}^3 r_{eo}\Gamma E_o e^{-\alpha_{RF} z} z}\, dz \quad (3)$$

The influence of various parameters on the resolution has been studied using numerical calculation of Eq. (3) in Matlab. These results are rendered in Fig. 4.

Fig. 4a shows the normalized optical intensity as a function of the output beam angle θ for different values of the leakage coefficient α_f by assuming the EO polymer optical losses of α_{opt} = 0.2 Np/cm (i.e., 1.74 dB/cm). The leaky light intensity increases with the leakage coefficient α_f. Indeed, for α_f = 0 Np/cm, the intensity of the leaky wave is zero because the lightwave is totally confined in the optical waveguide. But a high leakage coefficient leads to a larger beam divergence $\delta\theta$ by reducing effective waveguide length L_{eff} due to diffraction angle, as depicted in Fig. 4b. In fact, since the output beam divergence $\delta\theta$ is inversely proportional to L_{eff} with a

ACCEPTED MANUSCRIPT

higher leakage coefficient a larger beam divergence is to be experienced. It could be understood that increase in optical losses results also in an increase of the beam divergence via reduction of the effective waveguide length.

The results in Fig. 5 have been obtained with waveguide length L = 3 cm, optical losses α_{opt} = 0.2 Np/cm, RF losses α_{RF} = 0.01 Np/cm thanks to a pre-emphasis technique based on an appropriate modification of the gap between the strips of CPS electrode (to develop in detail in a coming paper), leaky coefficient α_f = 0.1 Np/cm, EO coefficient r_{eo} = 100 pm/V, overlap integral between the RF and optical fields Γ = 100%, applied voltage V = ± 20 V and gap of CPS line = 6 µm. The two peaks in Fig. 5.a correspond respectively to applied voltages V_{RF}= -20 V and +20 V, the spacing between them corresponds to the total angular sweeping Δθ. According to the curve in the Fig. 5.b, the number of resolvable lines is almost proportional to the EO coefficient of the core material. It has been easily demonstrated that the input voltage is linearly converted into spatial angular deflection.

4. Bandwidth

As mentioned above, the AOADC's resolution is proportional to the effective length of the EO deflector, while the modulation bandwidth is inversely proportional to the length L_{eff} due to the microwave and optical fields transit time mismatch limitations. To preserve the bandwidth, the deflector is designed to obtain the best velocity match possible between the optical and electrical waves. Indeed, if the velocities are matched, an optical pulse experiences the EO effect due to the input electrical RF field applied at the same instant throughout its propagation, and the leaky optical wave would be focused on even finer line. The maximum EO modulation frequency taking in account only the velocity mismatching is described by [12]:

$$f_{max} = \frac{2c}{\pi |n_{eff} - \sqrt{\varepsilon_{eff}}| L} \quad (4)$$

Where n_{eff} is the effective refractive index of the optical waveguide, ε_{eff} is the effective dielectric constant of the CPS line, L is the interaction length between optical and microwave fields, and c is the light velocity in free space.

According to equation (4), one should optimize the design of both optical and microwave structures of the EO deflector to make the effective refractive index n_{eff} and the square root of the effective dielectric constant ε_{eff} as close as possible to achieve broader bandwidth. When manufacturing, the deflector will be deposited on a silicon wafer, which serves as a popular substrate for Si Photonics combined with electronics (cf. Fig. 2), its high dielectric constant (ε_r =11.9) influences significantly the effective dielectric constant ε_{eff} and increase the difference between the effective refractive index and the square root of the effective dielectric constant, and hence, decrease the modulation bandwidth. To avoid this limitation, the electrical field must be isolated from the high dielectric constant of silicon by increasing the thickness of the lower cladding (h_g), with a lower dielectric constant.

All microwave features of the leaky waveguide have been calculated and optimized using the 3D full-wave electromagnetic field analysis software HFSS V. 15, such as characteristic impedance Z_o of the CPS line, effective dielectric constant ε_{eff} and microwave losses. Fig. 6 depicts the influence of the lower cladding thickness of NOA63 polymer (ε_r = 3.2, deposited on the silicon wafer of ε_r=11.9) on ε_{eff} and Z_o. As we can see, ε_{eff} varies from 5.6 to 4.1 when the

ACCEPTED MANUSCRIPT

lower cladding thickness varies from 10 to 100 μm. A thick lower cladding keeps the microwave signal away from the silicon substrate and allows ε_{eff} to get matched to the effective refractive index n_{eff} of 1.582. So the bandwidth can be improved.

Using travelling wave configuration, the EO deflector must be loaded with a resistor that matches the characteristic impedance of the electrodes. The CPS line is designed for a $Z_o = Z_L = 50\ \Omega$, where Z_L is the load impedance, and for velocity-matched bandwidth of over 20 GHz. Z_o depends not only on the geometric parameters of the CPS line but also all the surrounding materials. The gap G between CPS electrodes is fixed by the constraints of the optical waveguide manufacturing using micro-printing, core width of 3 μm and lateral claddings width of 3 μm, so G = 9 μm. Optimal electrode width is W = 350 μm, and the copper thickness t = 1 μm.

Compromises are made for achieving high bandwidth with required bit resolution in the design of the leaky waveguide deflector. The optimum length of L = 2.5 cm allows reaching the bandwidth of 20 GHz, for a thickness of the lower cladding of h_g = 100 μm (this provides an $\varepsilon_{eff} = 4.1$). An EO polymer with r_{eo} = 300 pm/V, which is below the state of the art of EO polymers [9], with an applied RF signal of magnitude V = ± 20 V (for a CPS gap = 6 μm at the input face of the waveguide and optimized over its length for electric field pre-emphasis) allows 6 bits of resolution for an optimum leaky coefficient of 0.1 Np/cm, corresponding to the buffet layer thickness of h_t = 3.75 μm. The leaky coefficient can be chosen higher than 0.1 Np/cm if we use higher EO coefficient. This allows increasing the bandwidth of the leaky waveguide deflector by reducing its length, and keeps the resolution to 6 bits.

5. Conclusion

A practical architecture of an all-optical spatial sampling ADC based on leaky waveguide deflector is presented. Optimum design of the central element of the AOADC, EO polymer leaky waveguide deflector, is reported here. The resulting sampling rate is 40 GS/s with 6 bits of resolution using available EO polymers, corresponding to a very high resolution-sampling rate product of 2.56×10^{12} LSBs-Hz. The current design takes into account the state of art of micro-printing manufacturing limits in our laboratories. Manufacturing and realization of this device are being addressed for experimental evaluations.

Accepted manuscript

Acknowledgement

The authors would like to thank the Region of Pays de la Loire for its support through the project ADC PolyNano. The authors appreciated helpful discussion and technical input of Prof. H. Gundel, Prof. B. Guiffard and Dr. S. Ginestar from IETR on micro-printing manufacturing limits.

References

[1] A.S. Daryoush, Digitally Beamformed Multibeam phased array antennas for future communication satellites, in Proceedings 2008 IEEE Radio and Wireless Symposium, Orlando USA, January 2008, pp. 831-834.

[2] Fujitsu Semiconductor Europe, Fujitsu Launches Second Generation Ultra-fast 65GSa/s 8-Bit ADC Technology for 100G Optical Transport, http://www.fujitsu.com/emea/news/pr/fseu-en_20100913-978.html#, (2010). http://www.eeweb.com/company-news/fujitsu_semiconductor/56-gsas-8-bit-adc-development-kit (2014)

ACCEPTED MANUSCRIPT

[3] M. El-Chammas, B. Murmann, A 12-GS/s 81-mW 5-bit time-interleaved flash ADC with background timing skew calibration, IEEE Journal of Solid-State Circuits, 46 (4), (2011), pp. 836-847.
[4] A. Khilo, S. J. Spector, M. E. Grein, A. H. Nejadmalayeri, C. W. Holzwarth, M. Y. Sander, M. S. Dahlem, M. Y. Peng, M. W. Geis, N. A. DiLello, J. U. Yoon, A. Motamedi, J. S. Orcutt, J. P. Wang, C. M. Sorace-Agaskar, M. A. Popovic, J. Sun, G.-R. Zhou, H. Byun, J. Chen, J. L. Hoyt, H. I. Smith, R. J. Ram, M. Perrott, T. M. Lyszczarz, E. P. Ippen, F. X. Kärtner, Photonic ADC: overcoming the bottleneck of electronic jitter, Optics Express, 20(4), (2012), pp. 4454‑4469.
[5] L. Hou, E. A. Avrutin, M. Haji, R. Dylewicz, A. C. Bryce, J. H. Marsh, 160 GHz Passively Mode-Locked AlGaInAs 1.55 μm Strained Quantum-Well Lasers With Deeply Etched Intracavity Mirrors, IEEE Journal of Selected Topics in Quantum Electronincs, 19 (4), (2013), 1100409.
[6] Y. Han, B. Jalali, Photonic time-stretched analog-to-digital converter: fundamental concepts and practical considerations, IEEE Journal of Lightwave Technology, Vol. 21 (12), (2003), pp. 3085-3103.
[7] Xiabo Hou, All-optical analog-to-digital converter up to 40 GSPS on spatial techniques, PhD Thesis, Drexel University, Philadelphia, PA, (2004).
[8] X. Zhang, A. Hosseini, X. Lin, H. Subbaraman, and R. T. Chen, Polymer-based hybrid integrated photonic devices for silicon on-chip modulation and board-level optical interconnects, IEEE Journal of Selected Topics in Quantum Electronics, 19(6), (2013), 3401115.
[9] S. Huang, T.-D. Kim, J. Luo, S. K. Hau, Z. Shi, X.-H. Zhou, H.-L. Yip, A. K.-Y. Jen, Highly efficient electro-optic polymers through improved poling using a thin TiO2-modified transparent electrode, Applied Physics Letters, 96 (24), (2010), pp. 243311: 1 - 3.
[10] D. Chen, H. R. Fetterman, A. Chen, W. H. Steier, L. R. Dalton, W. Wang, Y. Shi, Demonstration of 110 GHz electro-optic polymer modulators, Applied Physics Letters, 70 (25), (1997), pp. 3335-3337.
[11] G. Baili, M. Alouini, L. Morvan, D. Dolfi, A. Khadour, S. Bouchoule, J.-L. Oudar, Timing jitter reduction of a mode-locked VECSL using an optically triggered SESAM, IEEE Photonics Technology Letters, 22 (19), (2010), pp. 1434-1436.
[12] B. M. A. Rahman, V. Haxha, S. Haxha, K. T. V. Grattan, Design optimization of polymer electrooptic modulators, IEEE Journal of Lightwave Technology, 24 (9), (2006), pp. 3506-3513.

Figure captions:

Fig. 1. Conceptual diagram of the AOADC based on short-pulse laser for sampling, a leaky waveguide optical deflector and optical coding mask with array of photodiodes for quantization of applied RF signal.
Fig. 2. Cross section view of the optical leaky waveguide deflector on silicon substrate using EO polymer.
Fig. 3. (a) Predicted influence of the buffer layer thickness on the leaky wave coefficient with core refractive index n_c=1.63 and lower cladding and buffer layer refractive index n_g= n_t = 1.56 at the wavelength λ_o=1.55 μm. (b) Divergence angle of the leaky lightwave as function of the leakage coefficient.
Fig. 4. (a) Normalized optical intensity as a function of the output beam angle θ for different values of the leakage coefficient α_f. (b) Divergence angle of δθ for the leaky wave as a function of α_f.
Fig. 5. Simulations results obtained with L= 3 cm, α_{opt}= 0.2 Np/cm, α_{RF}= 0.01 Np/cm, α_f= 0.1 Np/cm, Γ=100%, V_{RF} = ± 20 V and CPS gap = 6 μm. (a) Leaky intensity peaks for applied voltages V_{RF} = -20 and +20 V with r_{eo} = 100 pm/V. (b) the number of resolvable lines as a function of EO coefficient.
Fig. 6. Influence of the lower cladding thickness on dispersion of CPS waveguide. (a) Effective relative permittivity. (b) Characteristic impedance.

Accepted manuscript

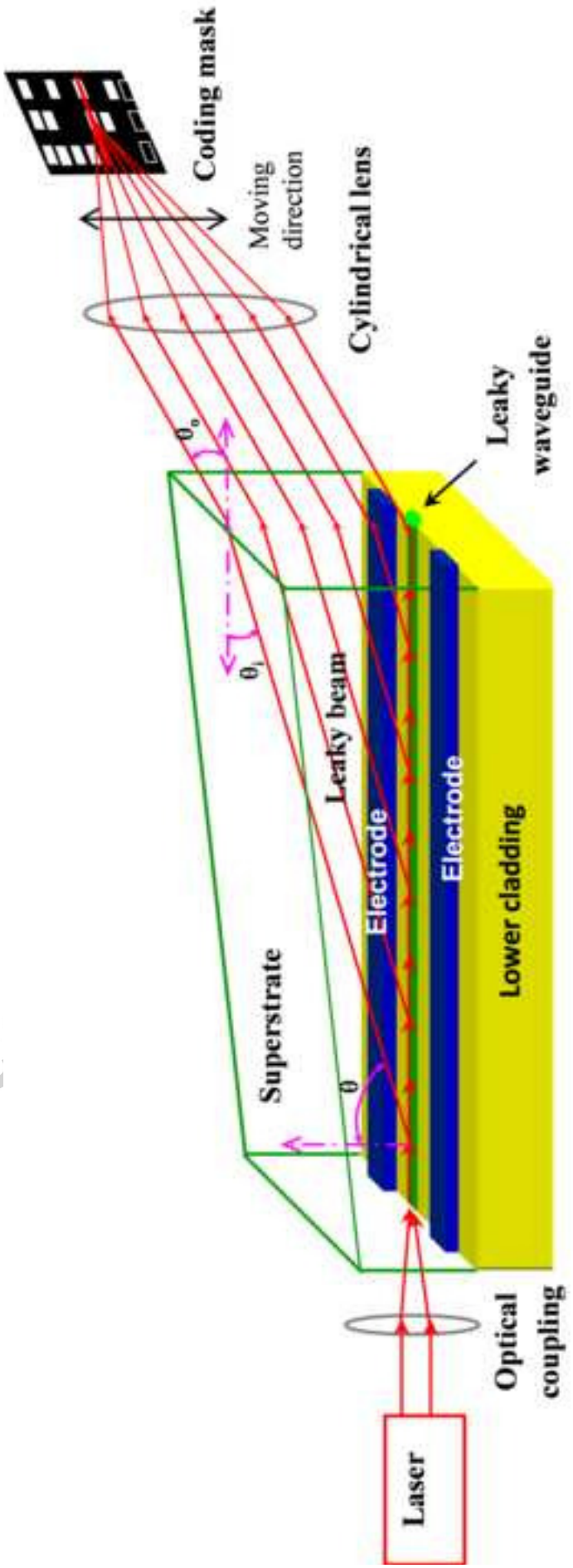
Coding mask
Moving direction
Cylindrical lens
Leaky waveguide
θ_o
θ_l
Leaky beam
Electrode
Electrode
Lower cladding
Superstrate
θ
Optical coupling
Laser

Figure(s)

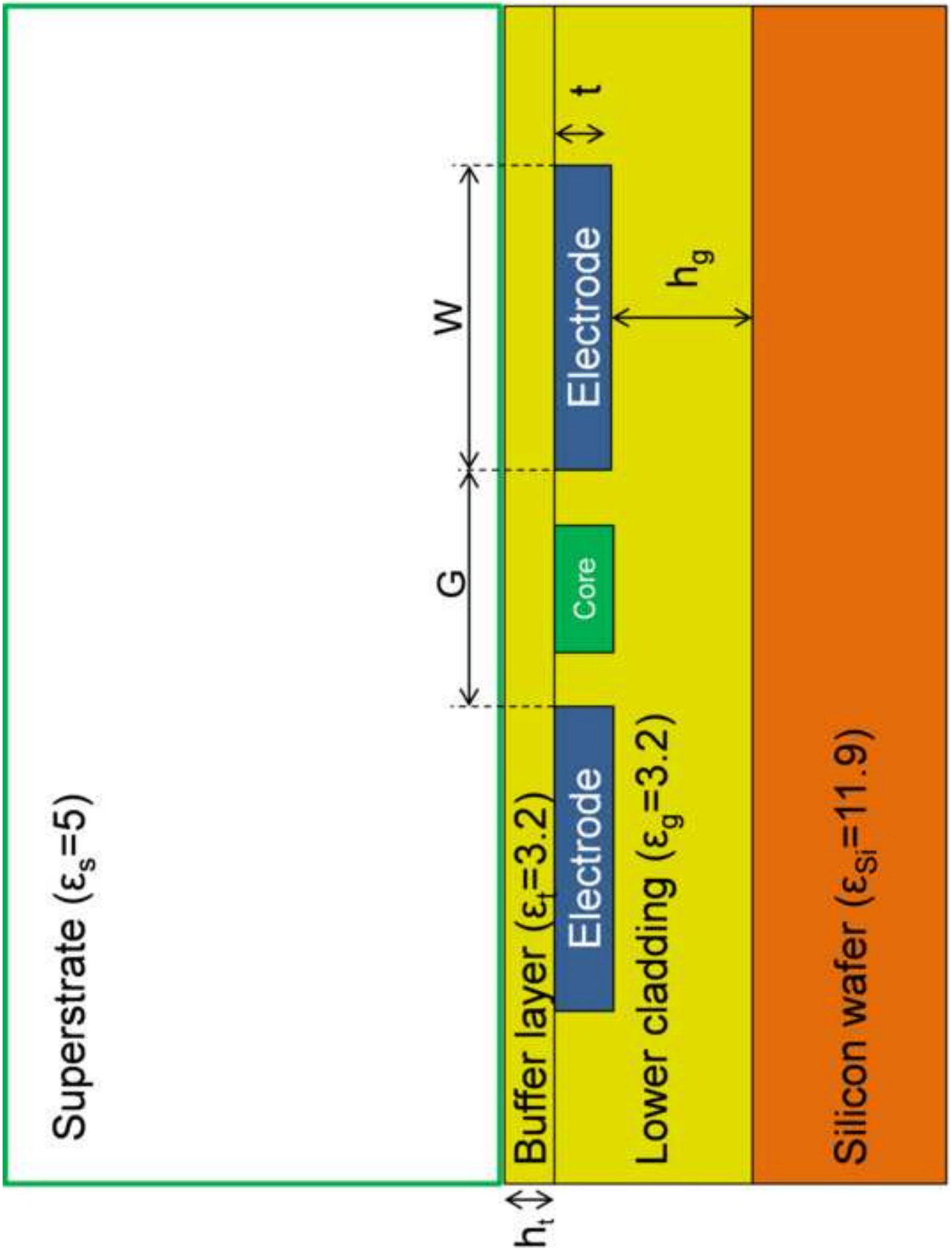
Superstrate (ε_s=5)
Buffer layer (ε_t=3.2)
Lower cladding (ε_g=3.2)
Silicon wafer (ε_{Si}=11.9)
Electrode
Core
Electrode
G
W
t
h_g
h_t

Figure2

ACCEPTED MANUSCRIPT

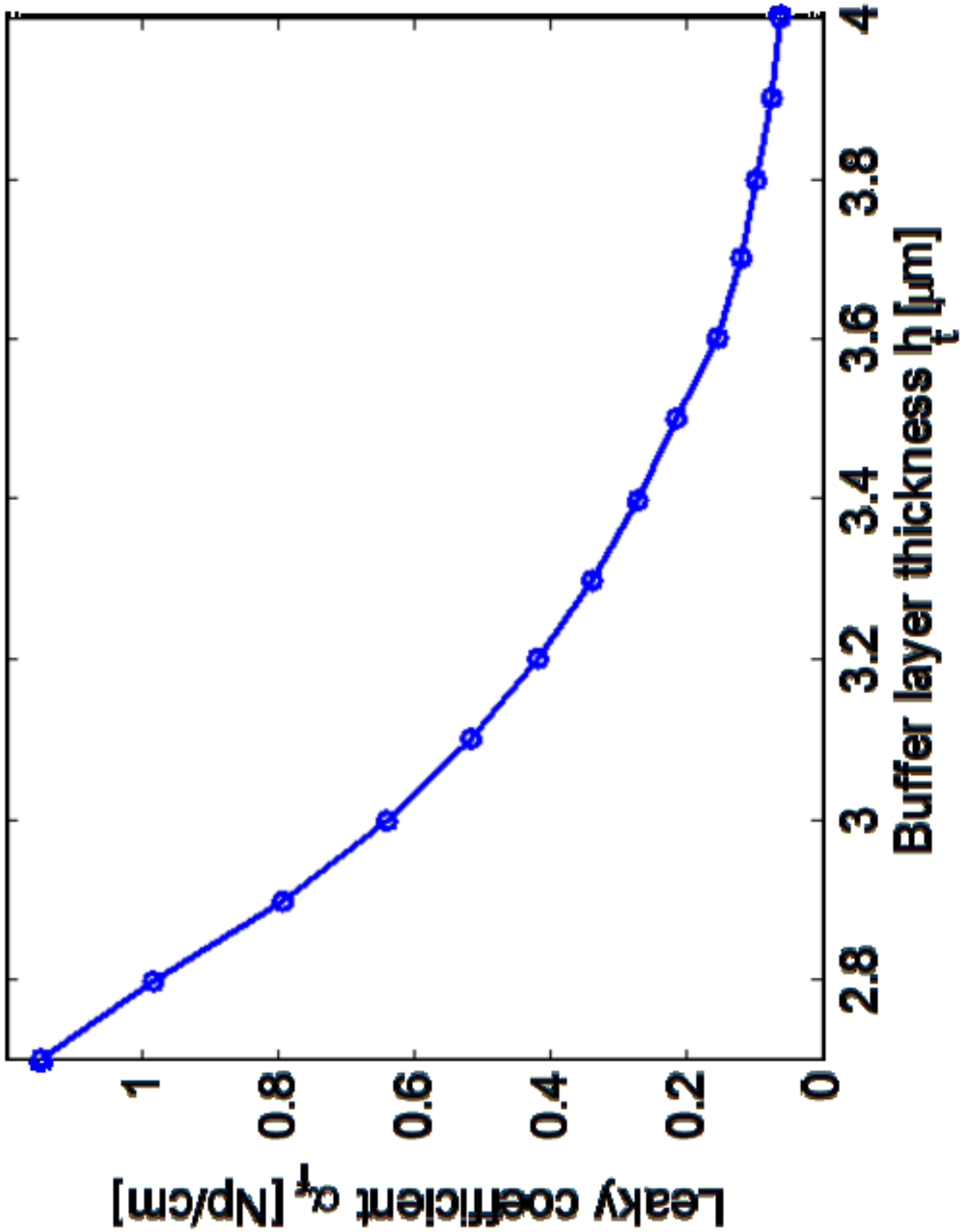

Figure3a

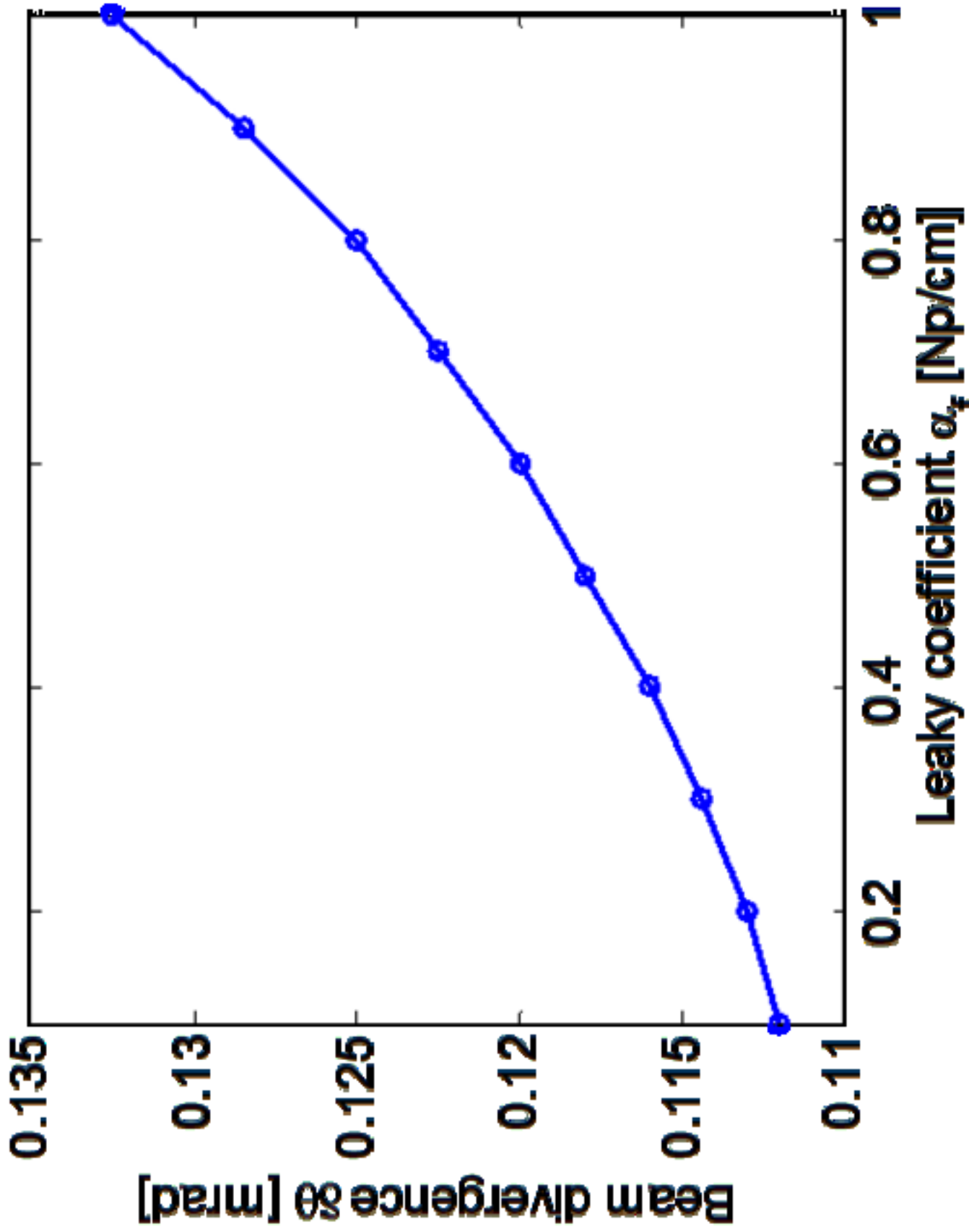
Beam divergence δθ [mrad]
0.135
0.13
0.125
0.12
0.115
0.11
0.2
0.4
0.6
0.8
1
Leaky coefficient α_f [Np/cm]

Figure3b

ACCEPTED MANUSCRIPT

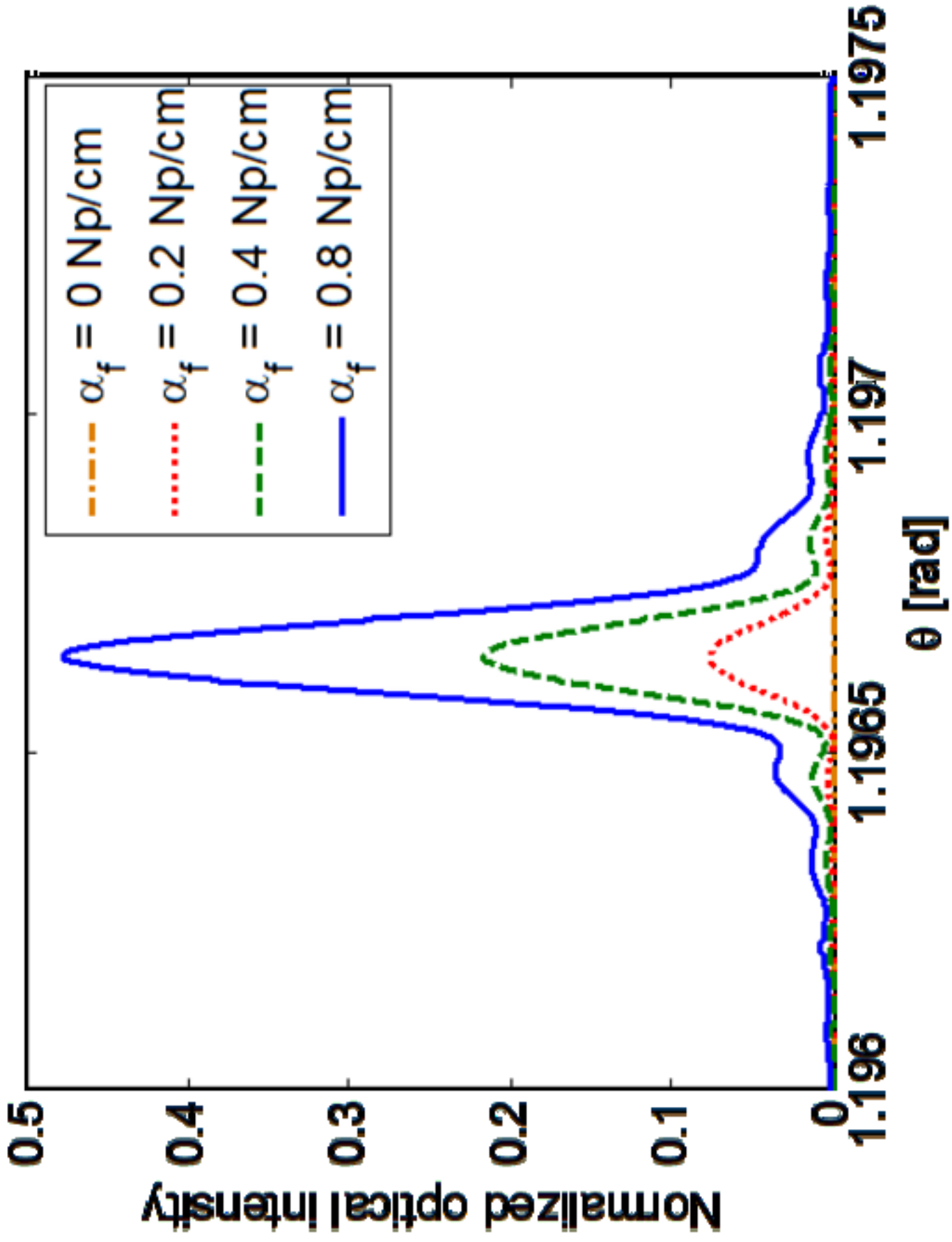

Figure4a

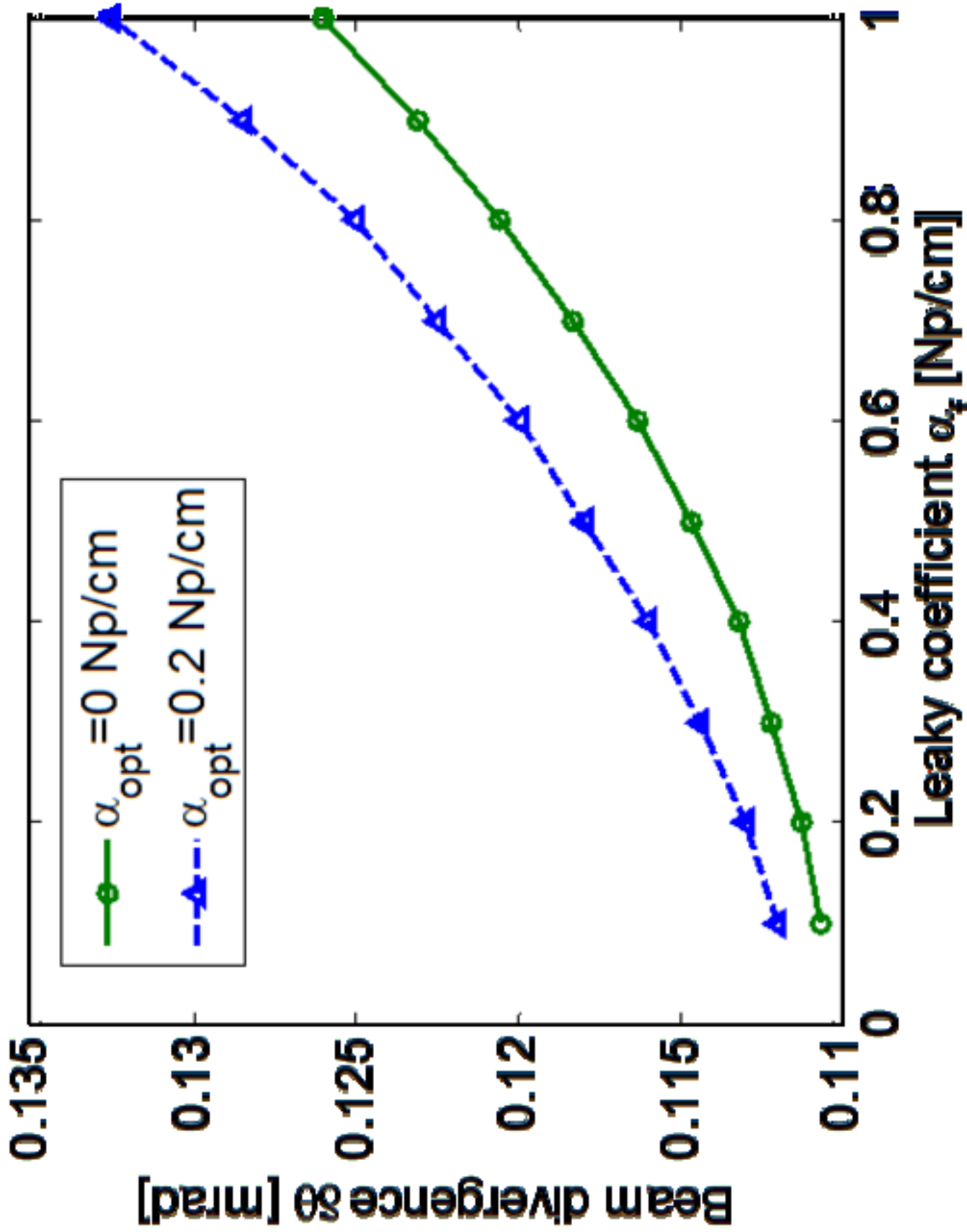
Beam divergence δθ [mrad]
0.135
0.13
0.125
0.12
0.115
0.11
0
0.2
0.4
0.6
0.8
1
Leaky coefficient α_f [Np/cm]
α_{opt}=0 Np/cm
α_{opt}=0.2 Np/cm

Figure4b

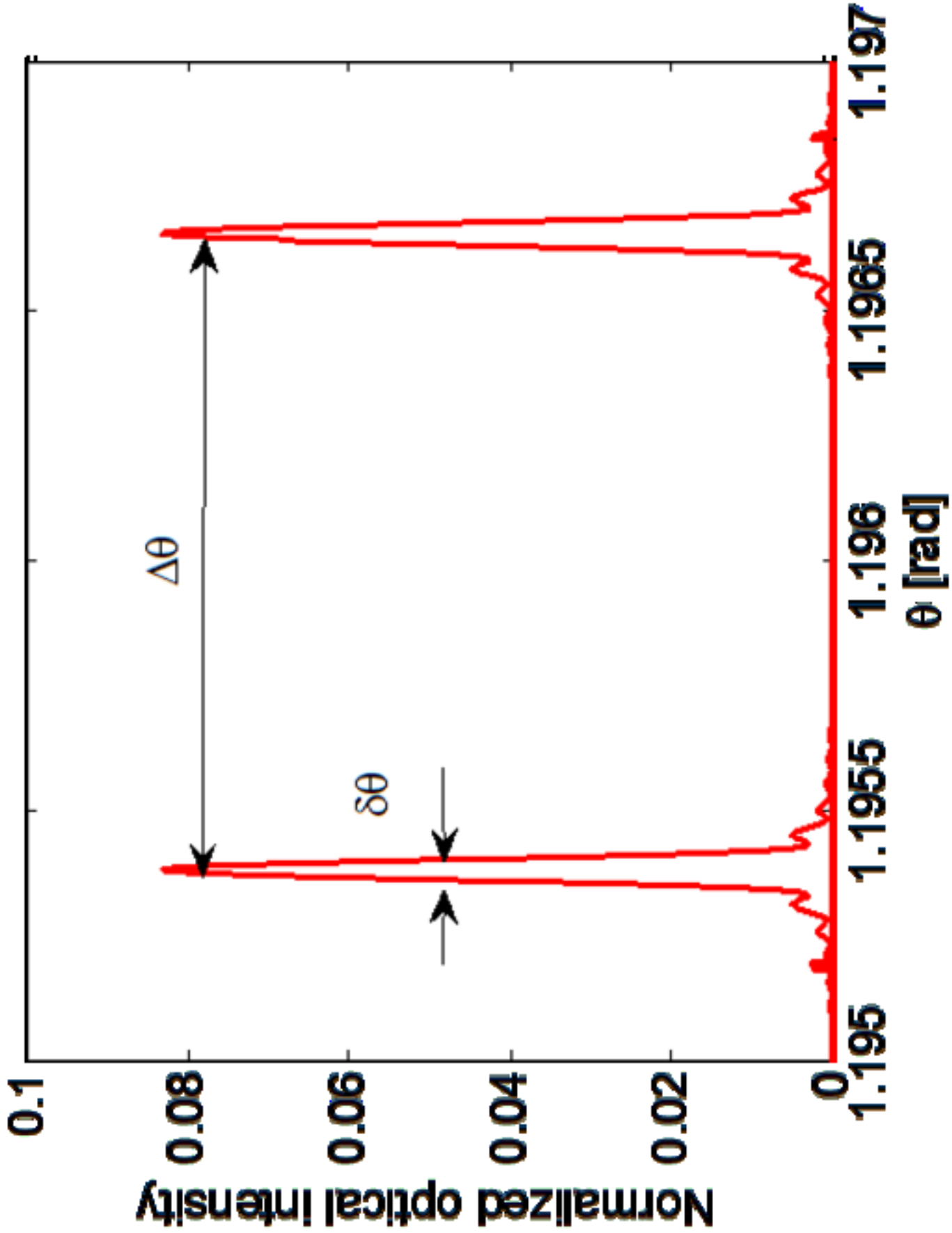
Normalized optical intensity
0.1
0.08
0.06
0.04
0.02
0
1.195
1.1955
1.196
1.1965
1.197
θ [rad]
Δθ
δθ

Figure5a

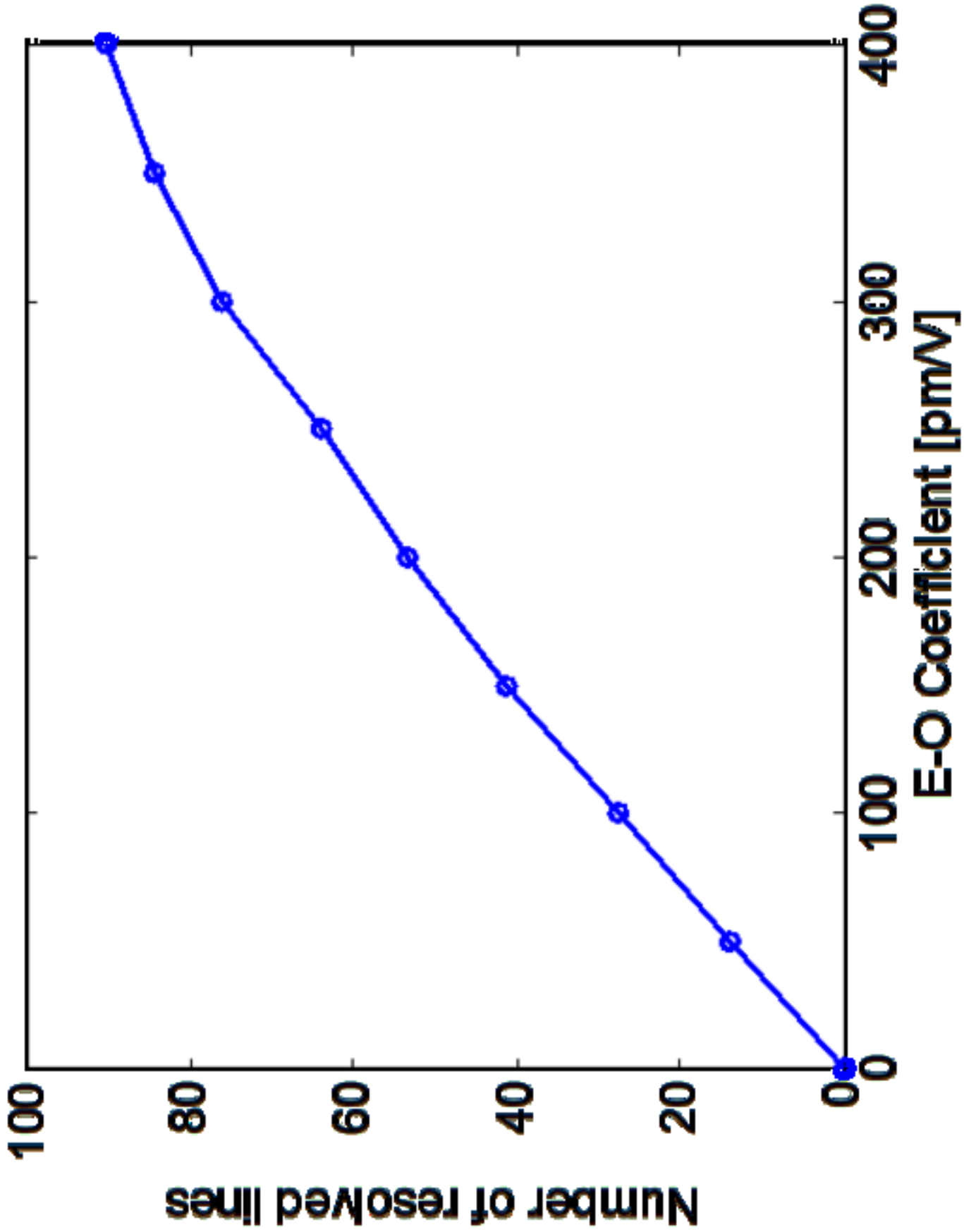
Number of resolved lines
E-O Coefficient [pm/V]
0
20
40
60
80
100
0
100
200
300
400

Figure5b

ACCEPTED MANUSCRIPT

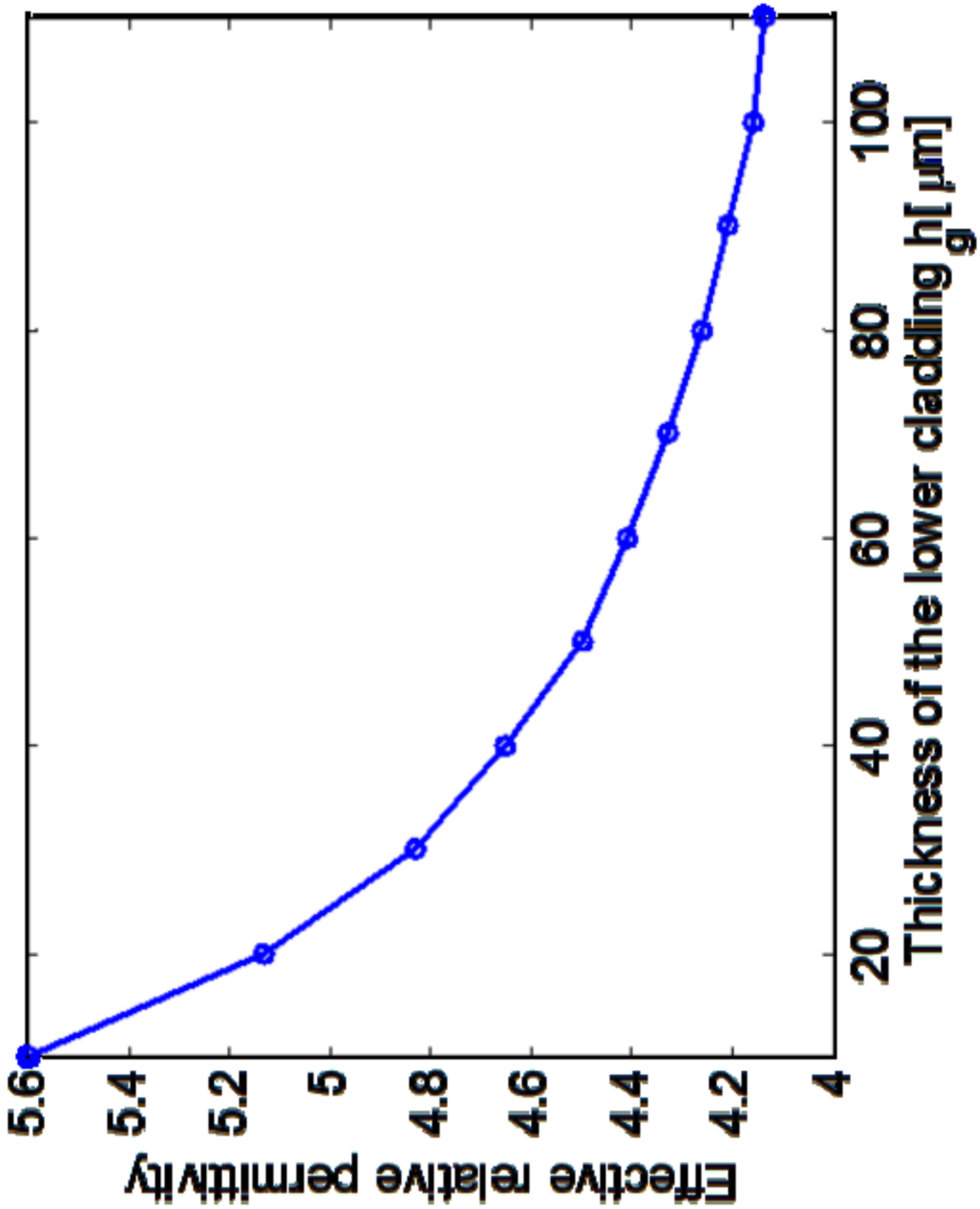

Figure6a

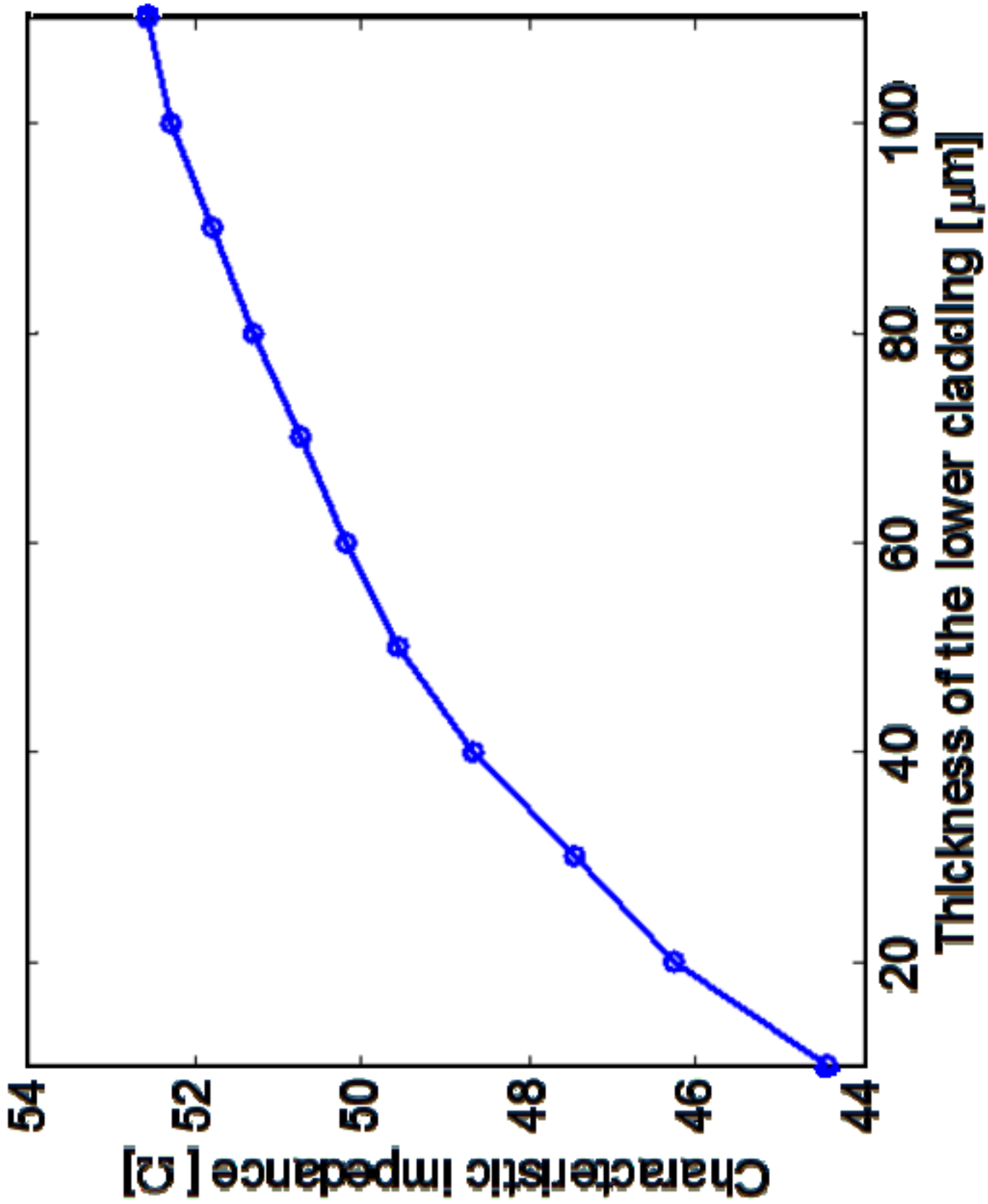
Characteristic impedance [Ω]
54
52
50
48
46
44
20
40
60
80
100
Thickness of the lower cladding [μm]

Figure6b